Monthly Notices of the ROYAL ASTRONOMICAL SOCIETY

MNRAS **452,** 3266–3272 (2015) doi:10.1093/mnras/stv1527

The *NuSTAR* X-ray spectrum of the low-luminosity active galactic nucleus in NGC 7213

F. Ursini,[1,2,3★] A. Marinucci,[3] G. Matt,[3] S. Bianchi,[3] A. Tortosa,[3] D. Stern,[4] P. Arévalo,[5] D. R. Ballantyne,[6] F. E. Bauer,[7,8,9] A. C. Fabian,[10] F. A. Harrison,[11] A. M. Lohfink,[10] C. S. Reynolds[12,13] and D. J. Walton[4,14]

[1] *Univ. Grenoble Alpes, IPAG, F-38000 Grenoble, France*
[2] *CNRS, IPAG, F-38000 Grenoble, France*
[3] *Dipartimento di Matematica e Fisica, Università degli Studi Roma Tre, via della Vasca Navale 84, I-00146 Roma, Italy*
[4] *Jet Propulsion Laboratory, California Institute of Technology, 4800 Oak Grove Drive, Mail Stop 169-221, Pasadena, CA 91109, USA*
[5] *Instituto de Física y Astronomía, Facultad de Ciencias, Universidad de Valparaíso, Gran Bretaña 1111, Playa Ancha, 2360102 Valparaíso, Chile.*
[6] *Center for Relativistic Astrophysics, School of Physics, Georgia Institute of Technology, Atlanta, GA 30332, USA*
[7] *Instituto de Astrofísica, Facultad de Física, Pontificia Universidad Católica de Chile, Casilla 306, Santiago 22, Chile.*
[8] *Millennium Institute of Astrophysics, Vicuña Mackenna 4860, 7820436 Macul, Santiago, Chile*
[9] *Space Science Institute, 4750 Walnut Street, Suite 205, Boulder, CO 80301, USA.*
[10] *Institute of Astronomy, University of Cambridge, Madingley Road, Cambridge CB3 0HA, UK*
[11] *Cahill Center for Astronomy and Astrophysics, California Institute of Technology, Pasadena, CA 91125, USA.*
[12] *Department of Astronomy, University of Maryland, College Park, MD 20742-2421, USA*
[13] *Joint Space-Science Institute (JSI), College Park, MD 20742-2421, USA*
[14] *Cahill Center for Astronomy and Astrophysics, California Institute of Technology, Pasadena, CA 91125, USA*

Accepted 2015 July 7. Received 2015 May 27; in original form 2015 April 17

ABSTRACT

We present an analysis of the 3–79 keV *NuSTAR* spectrum of the low-luminosity active galactic nucleus NGC 7213. In agreement with past observations, we find a lower limit to the high-energy cut-off of $E_c > 140$ keV, no evidence for a Compton-reflected continuum and the presence of an iron K α complex, possibly produced in the broad-line region. From the application of the MYTORUS model, we find that the line-emitting material is consistent with the absence of a significant Compton reflection if arising from a Compton-thin torus of gas with a column density of $5.0^{+2.0}_{-1.6} \times 10^{23}$ cm^{-2}. We report variability of the equivalent width of the iron lines on the time-scale of years using archival observations from *XMM–Newton*, *Chandra* and *Suzaku*. This analysis suggests a possible contribution from dusty gas. A fit with a Comptonization model indicates the presence of a hot corona with a temperature $kT_e > 40$ keV and an optical depth $\tau \lesssim 1$, assuming a spherical geometry.

Key words: galaxies: active – galaxies: individual: NGC 7213 – galaxies: Seyfert – X-rays: galaxies.

1 INTRODUCTION

The central engine of low-luminosity active galactic nuclei (LLAGNs) is thought to be powered by accretion of surrounding matter on to a supermassive black hole, similar to more powerful AGNs, like Seyfert galaxies and quasars (see Ho 2008, for a review). The X-ray spectrum of AGNs is generally dominated by a primary power-law component, which is thought to be produced by Comptonization of optical/UV photons emitted by the underlying accretion disc in a hot plasma, the so-called corona (see e.g. Haardt & Maraschi 1991; Haardt, Maraschi & Ghisellini 1994, 1997). A signature of this process is the presence of a high-energy cut-off in the X-ray emission, which has been observed in a number of sources (see e.g. Perola et al. 2002; Malizia et al. 2014; Brenneman et al. 2014; Ballantyne et al. 2014; Marinucci et al. 2014; Baloković et al. 2015; Ursini et al. 2015).

The distinctive characteristic of LLAGNs is their intrinsic faintness ($L_{bol} < 10^{44}$ erg s^{-1}). Moreover, the mass accretion rate of LLAGNs is generally small; in terms of the Eddington ratio, most of them have $L/L_{Edd} < 10^{-2}$ while luminous AGNs have $L/L_{Edd} \sim 0.01$–1 (see e.g. Panessa et al. 2006; Kollmeier et al. 2006). Whether LLAGNs are simply a scaled-down version of classical AGNs is a matter of debate. A standard geometrically thin, optically thick accretion disc (Shakura & Sunyaev 1973) may power LLAGNs (Maoz 2007), as is commonly assumed for

★ E-mail: francesco.ursini@obs.ujf-grenoble.fr

luminous AGNs. However, radiative-inefficient accretion flows (RIAFs; see e.g. Narayan & Yi 1994) have been proposed to explain some observational properties, in particular their lack of a UV bump (see e.g. Ho 2009; Yu, Yuan & Ho 2011). Furthermore, in luminous AGNs the hard X-ray photon index and the Eddington ratio are positively correlated (see e.g. Sobolewska & Papadakis 2009), while an anticorrelation is found in LLAGNs (Gu & Cao 2009). This result is consistent with the X-ray emission of LLAGNs originating from Comptonization in RIAFs, and it suggests a similarity between LLAGNs and black hole X-ray binaries (BHXRBs) in the low/hard state, where the accretion rate is low (Wu & Gu 2008). The low accretion rate might not only affect the structure of the inner accretion flow, but also that of the putative obscuring torus. The torus is predicted to disappear in low-luminosity sources by models depicting it as a clumpy wind, arising from the outer accretion disc (see e.g. Elitzur & Shlosman 2006, and references therein), or as a collection of many self-gravitating, dusty molecular clouds (see e.g. Hönig & Beckert 2007).

NGC 7213 is a nearby ($z = 0.005\,839$, as given in the NASA/IPAC Extragalactic Database; distance 25.80 Mpc; Pereira-Santaella et al. 2010) LLAGN with $L_{\rm bol} = 1.7 \times 10^{43}$ erg s^{-1} (Emmanoulopoulos et al. 2012) that hosts a supermassive black hole of $\sim 10^8$ solar masses (estimated from the stellar velocity dispersion, see Woo & Urry 2002), yielding an Eddington ratio of 1.4×10^{-3}. It has been historically classified as a Seyfert 1 because its optical spectrum shows broad emission lines, i.e. with a full width at half-maximum (FWHM) of a few thousand km s^{-1} (Phillips 1979). However, it has also been classified as a low-ionization nuclear emission region galaxy (LINER) because of the low excitation observed in the narrow-line spectrum (Filippenko & Halpern 1984). Low-ionization lines were also detected in the soft X-ray band (Starling et al. 2005). Wu, Boggess & Gull (1983) measured a UV flux higher than the extrapolated optical flux, thus indicating a possible UV bump, but it is still weaker than in most Seyfert galaxies. More recently, Starling et al. (2005) found no evidence for an optical/UV bump using *XMM–Newton*/OM data.

The X-ray spectrum of NGC 7213 shows peculiarities as well. The Compton reflection component is found to be weak or absent with *XMM–Newton*, *BeppoSAX* and *Suzaku* observations (see e.g. Bianchi et al. 2003; Lobban et al. 2010), in contrast to what is commonly observed in Seyfert 1 galaxies. This may suggest that the accretion disc is truncated in the inner region, perhaps replaced by a Compton-thin RIAF (Lobban et al. 2010). An iron line complex is clearly detected between 6.4 and 7 keV, consisting of three narrow K α emission lines respectively from neutral Fe, Fe XXV and Fe XXVI (see e.g. the analysis of *Chandra* data by Bianchi et al. 2008). Given the lack of an observed Compton reflection hump, such lines cannot originate from Compton-thick material, like the accretion disc or a parsec-scale torus. Bianchi et al. (2008) found the FWHM of the neutral Fe K α line to be consistent with that of the H α line ($\sim$2600 km s^{-1}), thus suggesting a common origin in the broad-line region (BLR). Another possibility is reprocessed emission from dusty gas, which can produce strong, neutral Fe K α emission with a weak associated continuum (Gohil & Ballantyne 2015). Emmanoulopoulos et al. (2012) found an anticorrelation between the X-ray photon index and the X-ray luminosity that, together with the low accretion rate of the source, indicates a spectral behaviour similar to that of BHXRBs in the hard state. Finally, Bianchi et al. (2003) reported a high-energy cut-off of 95^{+75}_{-45} keV using *XMM–Newton*+*BeppoSAX* data, while Lobban et al. (2010) found a lower limit of 350 keV using *Suzaku*/XIS+PIN and *Swift*/BAT data.

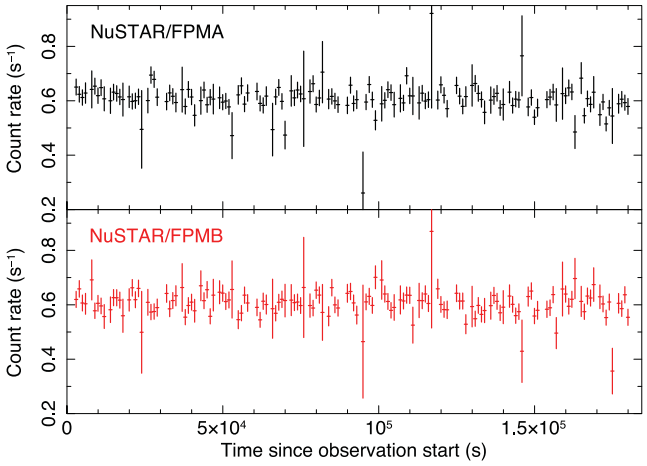

Figure 1. The *NuSTAR*/FPMA and FPMB 3–79 keV light curve. Bins of 1000 s are used.

In this paper, we report on a *NuSTAR* observation of NGC 7213 performed in 2014 October. The primary focus of this work is modelling the broad-band X-ray spectrum of the source and constraining the origin of the X-ray emission. In Section 2, we describe the observations and data reduction. In Section 3, we present the analysis of the 3–79 keV spectrum, fitted with both a phenomenological and a realistic Comptonization model, and we study the time evolution of the iron line complex by analysing archival *XMM–Newton*, *Chandra* and *Suzaku* data. In Section 4, we discuss the results and summarize our conclusions.

2 OBSERVATIONS AND DATA REDUCTION

NuSTAR (Harrison et al. 2013) observed NGC 7213 starting on 2014 October 5, with a net exposure of 109 ks (Obs. Id. 60001031002). The *NuSTAR* data were reduced with the standard pipeline (NUPIPELINE) in the *NuSTAR* Data Analysis Software (NUSTARDAS, v1.3.1; part of the HEASOFT distribution as of version 6.14), using calibration files from *NuSTAR* CALDB v20141107. Spectra and light curves were extracted from the cleaned event files using the standard tool NUPRODUCTS for each of the two hard X-ray telescopes aboard *NuSTAR*, which have corresponding focal plane modules A and B (FPMA and FPMB). The spectra from FPMA and FPMB are analysed jointly, but are not combined, allowing for a free cross-calibration constant. The source data were extracted from circular regions (radius 75 arcsec), and background was extracted from a blank area close to the source. Finally, the spectra were binned to have a signal-to-noise ratio greater than 3 in each spectral channel, and not to oversample the instrumental resolution by a factor greater than 2.5.

In Fig. 1, we show the *NuSTAR*/FPMA and FPMB light curves obtained in the 3–79 keV energy range. The total variation in the light curve is of the order of a few per cent. Therefore, in the following we analyse the time-averaged spectrum of the source.

3 SPECTRAL ANALYSIS

Spectral analysis and model fitting was carried out with the XSPEC 12.8 package (Arnaud 1996), using the χ^2 minimization technique throughout. In this work, the errors are quoted at the 90 per cent confidence level, if not stated otherwise.

Table 1. Best-fitting parameters of the baseline model including a primary cut-off power law and three Gaussian lines (line 1 at 6.4 keV, line 2 at 6.7 keV, line 3 at 6.966 keV).

Γ	1.84 ± 0.03
E_c (keV)	>140
$F_{3-10keV}$ (10^{-11} erg cm^{-2} s^{-1})	1.3 ± 0.1
EW$_1$ (eV)	98^{+30}_{-20}
F_1 (10^{-5} ph cm^{-2} s^{-1})	$1.7^{+0.3}_{-0.4}$
EW$_2$ (eV)	29^{+24}_{-18}
F_2 (10^{-5} ph cm^{-2} s^{-1})	$0.5^{+0.5}_{-0.3}$
EW$_3$ (eV)	42 ± 20
F_3 (10^{-5} ph cm^{-2} s^{-1})	0.6 ± 0.3
χ^2/d.o.f.	375/366

3.1 The *NuSTAR* spectrum

As a first step, we define a phenomenological model, which we describe below. We fit the *NuSTAR* data in the 3–79 keV range, allowing for a free cross-calibration constant between the modules FPMA and FPMB. The two modules are in good agreement, with a cross-calibration factor $K_{A-B} = 0.99 \pm 0.01$ fixing the constant for the FPMA data to unity.

We modelled the continuum with a cut-off power law, modified by neutral absorption (PHABS model in XSPEC) from Galactic hydrogen with column density $N_H = 2.04 \times 10^{20}$ cm^{-2} (Dickey & Lockman 1990). This simple model yields a poor fit (reduced $\chi^2 = 556/369$), with positive residuals between 6 and 7 keV, which can be attributed to the known Fe complex between 6.4 and 7 keV (Bianchi et al. 2003, 2008). Bianchi et al. (2008) found three emission lines in the *Chandra*/HEG spectrum, at 6.4, 6.7 and 6.966 keV. These lines are interpreted as emission from neutral Fe, Fe XXV and Fe XXVI, respectively. *Chandra*/HEG data provide much higher energy resolution near the Fe complex compared with *NuSTAR*. We thus followed the analysis of Bianchi et al. (2008) and tested for the presence of three narrow Gaussian lines fixing their energies at 6.4, 6.7 and 6.966 keV, leaving the normalizations free to vary. The inclusion of a narrow Gaussian line at 6.4 keV yields a significantly improved fit (reduced $\chi^2 = 417/368$). Adding a second line at 6.7 keV further improves the fit (reduced $\chi^2 = 388/367$), with a probability of chance improvement less than 4×10^{-7} according to the *F*-test. The inclusion of a third line at 6.966 keV yields a good fit (reduced $\chi^2 = 375/367$), without prominent residuals and a probability of chance improvement less than 5×10^{-4} according to the *F*-test.

We report the results of this fit in Table 1, and in Fig. 2 we show the contour plots of the cut-off energy versus photon index. In Fig. 3, we show the data, residuals and best-fitting model. To further test the presence of a high-energy cut-off, we included the 70-month average *Swift*/BAT spectrum (Baumgartner et al. 2013); however, the results are essentially unchanged.

We tested for the presence of a reflection continuum by including the PEXRAV model in XSPEC, which describes neutral Compton reflection of infinite column density in a slab geometry (Magdziarz & Zdziarski 1995). This model is adequate for reflection off a standard accretion disc, given the high column densities expected for these structures (see e.g. Svensson & Zdziarski 1994). We fixed the inclination angle of the reflector to 30 deg, appropriate for a type 1 source (e.g. Nandra et al. 1997). The photon index and cut-off energy of the incident spectrum were tied to those of the primary power law. However, no improvement is found, with only

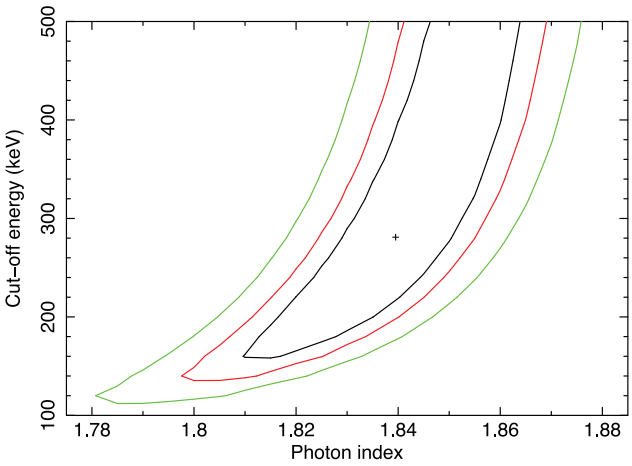

Figure 2. Primary continuum cut-off energy versus photon index contours. Solid green, red and black lines correspond to 99, 90 and 68 per cent confidence levels, respectively.

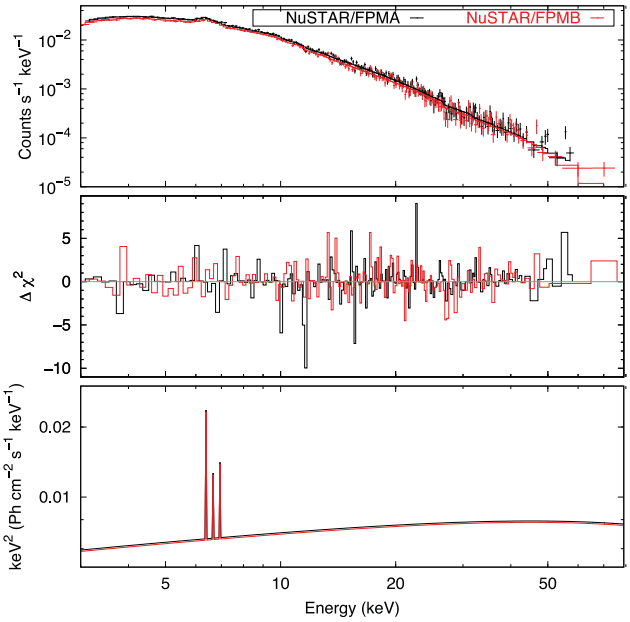

Figure 3. The *NuSTAR* spectrum and baseline model (see Table 1). Upper panel: *NuSTAR* data and folded model. Middle panel: contribution to χ^2. Lower panel: best-fitting model $E^2f(E)$ with the plot of the additive components, namely the cut-off power law and the three Fe K α lines.

an upper limit to the reflection fraction $\mathcal{R}$ of 0.13, at 90 per cent confidence level. In Fig. 4, we show the contour plots of $\mathcal{R}$ versus photon index. This is consistent with the iron lines originating from Compton-thin material ($N_H = 10$–10^{23} cm^{-2}), which does not produce a prominent Compton reflection hump (Bianchi et al. 2003). To test this result further, we replaced the PEXRAV component and the neutral Fe K α line with the MYTORUS model, which includes Compton reflection and iron fluorescent lines from a gas torus with an opening angle of 60 deg (Murphy & Yaqoob 2009). The inclination angle of the torus was fixed at 30 deg. The column densities of the scattered and line components were linked and free to vary. The normalizations of the scattered and line components were tied to the normalization of the primary power law, i.e. the standard MYTORUS configuration ('coupled' reprocessor; see e.g. Yaqoob 2012). The assumed geometry corresponds to a covering fraction

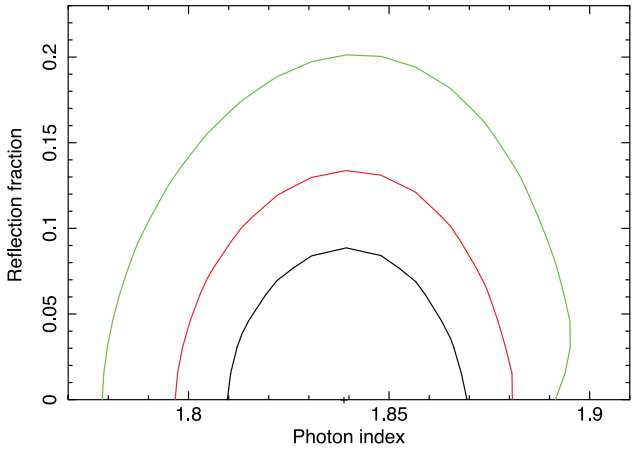

Figure 4. PEXRAV reflection fraction versus photon index contours. Solid green, red and black lines correspond to 99, 90 and 68 per cent confidence levels, respectively.

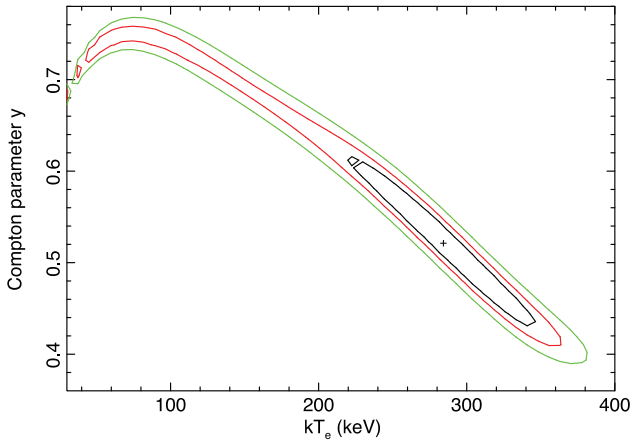

Figure 5. COMPPS Compton parameter versus temperature contours. Solid green, red and black lines correspond to 99, 90 and 68 per cent confidence levels, respectively.

of 0.5. We obtain a good fit (reduced $\chi^2 = 373/363$) and we find a column density of $5.0^{+2.0}_{-1.6} \times 10^{23}$ cm^{-2}. This result is consistent with the estimate of $\sim 3 \times 10^{23}$ cm^{-2} for the Fe K α line-emitting material reported in Bianchi et al. (2008).

We next replaced the cut-off power law with the Comptonization model COMPPS (Poutanen & Svensson 1996) in XSPEC. COMPPS models the thermal Comptonization emission of a hot plasma cooled by soft photons with a disc blackbody distribution. We set a spherical geometry (parameter GEOM $= -4$ in COMPPS) for the hot plasma and a temperature at the inner disc radius of 10 eV, fitting for the electron temperature kT_e and Compton parameter $y = 4\tau(kT_e/m_ec^2)$. The model yields a good fit (reduced $\chi^2 = 375/366$) with best-fitting parameters $kT_e = 295^{+70}_{-250}$ keV and $y = 0.52^{+0.34}_{-0.10}$, which imply an optical depth $\tau = 0.2^{+0.7}_{-0.1}$. In Fig. 5, we show the kT_e–y contour plots.

3.2 Time evolution of the Fe K α line

To try to understand the origin of the Fe K α lines, we compared our results with past observations of NGC 7213 by re-analysing the archival *XMM–Newton* (2001, 2009), *Chandra* (2007) and *Suzaku* (2006) data. We fitted the 3–10 keV data sets with the baseline

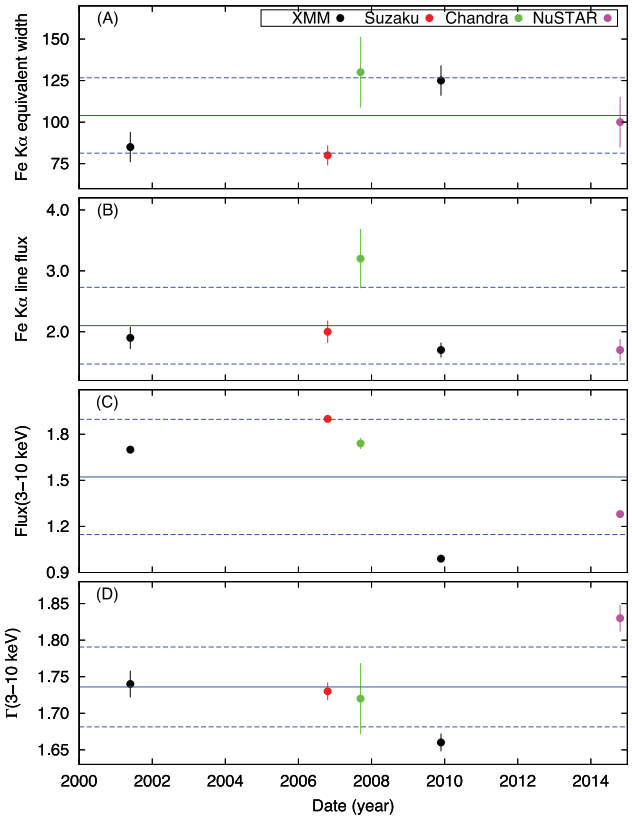

Figure 6. Time evolution of Fe K α line parameters and 3–10 keV primary flux and photon index. Panel (A): Fe K α equivalent width in eV units. Panel (B): Fe K α line flux in units of 10^{-5} photons cm^{-2} s^{-1}. Panel (C): continuum 3–10 keV flux in units of 10^{-11} erg cm^{-2} s^{-1}. Panel (D): 3–10 keV photon index. Error bars denote the 1σ uncertainty. The blue solid lines represent the mean value for each parameter, while the blue dashed lines correspond to the standard deviation.

model described in Section 3.1, i.e. including a cut-off power law and three narrow Gaussian lines. The best-fitting parameters are consistent with those reported in Bianchi et al. (2003, 2008) and Lobban et al. (2010).

In Fig. 6, we show the time evolution of the neutral Fe K α line EW and flux, and of the 3–10 keV continuum flux and photon index. The continuum flux variations reach up to a factor of 2, while the line flux varies at the 1σ confidence level only during the *Chandra*/HEG observation of 2007. The line EW, on the other hand, exhibits significant variations up to a factor of 1.7. The data show a hint of an anticorrelation between the continuum flux and the line EW, though we cannot formally establish a significant relation. The Spearman rank correlation coefficient is -0.4, but the test returns a P value of 0.42, implying that the null hypothesis is not rejected. Similar results hold for the Fe XXV and Fe XXVI lines, albeit with larger uncertainties on their parameters.

4 DISCUSSION AND CONCLUSIONS

We reported results based on a *NuSTAR* observation of the LLAGN/LINER NGC 7213. We derived constraints on the parameters describing the high-energy (3–79 keV) spectrum, and studied variability over a few year time-scale comparing our results with archival observations of the source.

We have been able to constrain the reflection component, finding no evidence for a significant Compton reflection continuum.

This is consistent with previous results (e.g. Bianchi et al. 2003; Lobban et al. 2010; Emmanoulopoulos et al. 2013). We note that the constraints on the reflection component are derived assuming a static X-ray source (Magdziarz & Zdziarski 1995; Murphy & Yaqoob 2009), but it may actually be outflowing (Beloborodov 1999; Malzac, Beloborodov & Poutanen 2001). An outflowing, energetically dominant corona can be generated by a geometrically thin, optically thick accretion disc at low accretion rates (Merloni & Fabian 2002). This scenario is consistent with the lack of a significant optical/UV bump from the disc, if the power output is dominated by the corona. Furthermore, an outflowing X-ray corona could account for the absence of a disc reflection component, since the primary emission would be beamed away from the disc. This has been suggested especially for radio-loud sources having relativistic jets, where the X-ray corona might be the base of the jet itself (see e.g. Lohfink et al. 2013; Walton et al. 2013; Ballantyne et al. 2014; Fabian et al. 2014). Although NGC 7213 is a radio-intermediate source with no clear evidence for a strong jet (Blank, Harnett & Jones 2005; Bell et al. 2011), its radio emission is found to be weakly correlated with the X-ray emission (Bell et al. 2011). Therefore, the outflowing corona scenario cannot be ruled out in this source.

We confirm the presence of an iron complex between 6.4 and 7 keV (Bianchi et al. 2003), consisting of three narrow K α emission lines from neutral Fe, Fe XXV and Fe XXVI. The lack of a Compton reflection hump above 10 keV indicates that these lines cannot originate from Compton-thick material. Using the MYTORUS self-consistent model, we find that the neutral Fe K α line may be produced by material with a covering fraction of 0.5 and a column density of $5.0^{+2.0}_{-1.6} \times 10^{23}$ cm^{-2}. This result is consistent with the iron line complex being produced in the BLR (Bianchi et al. 2008). Assuming that the line widths represent a Keplerian velocity, it is possible to estimate the distance of the BLR using the virial theorem, i.e. $R_{\rm pc} \simeq 4.5 \times 10^5 f^{-1} M_8 (\Delta V_{\rm km\,s^{-1}})^{-2}$, where $R_{\rm pc}$ is the distance in units of parsecs, f is a coefficient that accounts for the unknown geometry and orientation (Peterson et al. 2004), M_8 is the black hole mass in units of 10^8 solar masses and $\Delta V_{\rm km\,s^{-1}}$ is the line width in units of km s^{-1}. Bianchi et al. (2008) report an FWHM of 2400^{+1100}_{-600} km s^{-1} for the neutral Fe K α line using the *Chandra*/HEG data, and 2640^{+110}_{-90} km s^{-1} for the H α line using ESO-NTT optical data. Setting $f = 4.3$ (Grier et al. 2013), the virial theorem yields a BLR distance of $\sim$0.02 pc. Alternatively, reprocessing may occur in dusty gas, since the presence of dust may enhance the neutral Fe K α EW (Gohil & Ballantyne 2015). This effect is due to a suppression of the reflected continuum, caused by the reduction of backscattering opacity in dusty gas (Draine 2003). This hypothesis is supported by the presence of strong silicate emission features in the mid-IR spectrum of NGC 7213 (Hönig et al. 2010; Ruschel-Dutra et al. 2014). The dust sublimation radius is estimated to be $\sim$0.03 pc from the optical luminosity (Hönig et al. 2010). Therefore, if the line originates from dusty gas, the line-emitting region should be more distant than the BLR, as suggested by the constancy of the line flux on a few year time-scale (see below). We also note that the lack of any cold reflection from Compton-thick material is consistent with the models of clumpy tori, which are predicted to disappear in low-luminosity sources (Elitzur & Shlosman 2006; Hönig & Beckert 2007).

We analysed the neutral Fe K α line time evolution over $\sim$15 years by re-fitting archival *XMM–Newton*, *Suzaku* and *Chandra* data of the source. According to our estimate, the BLR distance is $\sim$0.02 pc, or $\sim$20 light days (see also Kaspi et al. 2005; Balmaverde & Capetti 2014). The observed X-ray variability time-scale of NGC 7213 is of several days or weeks (Emmanoulopoulos et al. 2012), in agreement with the lack of variability during the $\sim$100 ks *NuSTAR* observation. We would thus expect the Fe K α line flux to vary in response to the continuum variations, albeit with a time delay due to the light-travel time. However, we only detect a marginal variability of the line flux during the *Chandra* observation of 2007. Therefore, a contribution from more distant material cannot be ruled out. The *Astro-H* satellite, providing an unprecedented combination of high spectral resolution and effective area at 6–7 keV, will likely enable us to solve the ambiguous origin of the Fe K α line. For example, the line might be the superposition of two components, namely a broad component from the BLR and a narrow one produced further away, which *Astro-H* should be able to disentangle (Reynolds et al. 2014).

The primary continuum is well fitted by a power law with a photon index $\Gamma = 1.84 \pm 0.03$, and an extrapolated 2–10 keV flux $F_{2-10} = (1.6 \pm 0.1) \times 10^{-11}$ erg cm^{-2} s^{-1}. The 3–10 keV continuum flux and photon index that we found for the archival observations do not show a clear trend (see Fig. 6). The extrapolated 2–10 keV luminosity is $L_{2-10} = (1.2 \pm 0.1) \times 10^{42}$ erg s^{-1}. Using the 2–10 keV bolometric correction of Marconi et al. (2004), we estimate the bolometric luminosity to be $L_{\rm bol} = (1.3 \pm 0.1) \times 10^{43}$ erg s^{-1}. For a black hole mass of 10^8 M$_\odot$, the Eddington luminosity is 1.2×10^{46} erg s^{-1}. These estimates yield an accretion rate of $\sim$0.1 per cent of the Eddington limit, in rough agreement with the value of 0.14 per cent by Emmanoulopoulos et al. (2012) based on the broad-band spectral energy distribution. An Eddington ratio $\sim 10^{-3}$ is lower than what is typically found for luminous AGNs, namely $\sim 0.01 - 1$, and it lies within the theoretically predicted RIAF regime (Narayan, Mahadevan & Quataert 1998; Ho 2009).

We can only place a lower limit on the presence of a high-energy cut-off, $E_{\rm c} > 140$ keV, consistent with the lower limit of 350 keV found by Lobban et al. (2010) using *Suzaku*+*Swift*/BAT data, and marginally consistent with the value of 95^{+75}_{-45} keV found by Bianchi et al. (2003) using *XMM–Newton*+*BeppoSAX* data. Replacing the cut-off power law with a Comptonization model and assuming a spherical geometry, we estimate the coronal temperature to be >40 keV ($kT_{\rm e} = 295^{+70}_{-250}$ keV) and we measure an optical depth $\tau = 0.2^{+0.7}_{-0.1}$. The lack of an upper limit on the high-energy cut-off does not conflict with the upper limit on the coronal temperature, because a cut-off power law is known to be a rough approximation of Comptonization models (see e.g. Stern et al. 1995). First, the high-energy turnover of a Comptonization spectrum is much sharper than an exponential cut-off (see e.g. Zdziarski et al. 2003). Moreover, a Comptonization spectrum is actually a superposition of several orders of Compton scattering spectra. When the optical depth is small, the different scattering orders are separated in energy, thus resulting in a bumpy spectral shape (see e.g. Poutanen & Svensson 1996). But the optical depth and temperature are inversely related for a given heating/cooling ratio, i.e. the ratio of the power dissipated in the corona to the intercepted soft luminosity (Stern et al. 1995; Haardt et al. 1997). This can produce an upper limit on the coronal temperature even if no exponential cut-off is required (see e.g. Petrucci et al. 2013).

The combination of a weak or absent reflected continuum, a weak UV bump and a low accretion rate suggest that the standard optically thick, geometrically thin accretion disc is truncated in the inner region of the source (Starling et al. 2005; Lobban et al. 2010). A possible explanation is that the nucleus accretes via a RIAF, with the inner edge of any standard disc restricted to large distances, $\sim 10^2$ gravitational radii (see e.g. Quataert et al. 1999). This is a natural suggestion for an LLAGN, since RIAFs are only

expected in sub-Eddington systems and the low radiative efficiency would explain the observed low luminosity. The X-ray emission from an RIAF is likely dominated by thermal Comptonization, in agreement with observations of X-ray binaries in the hard state (see e.g. Narayan 2005, and references therein). The soft seed photons can be synchrotron photons produced in the hot accretion flow itself (synchrotron self-Compton), or thermal photons from the outer thin disc (see e.g. Yuan & Zdziarski 2004; Nemmen, Storchi-Bergmann & Eracleous 2014). As we noted above, the X-ray variability timescale of NGC 7213 is of the order of days/weeks (Emmanoulopoulos et al. 2012). Therefore, the Comptonization process is consistent with taking place in an extended region with $kT_e > 40$ keV and $\tau \lesssim 1$, possibly illuminated by the outer thin disc. The relatively small optical depth is a further indication that the corona should be extended and subtend a large solid angle as seen from the disc, in order to scatter a sufficient number of soft photons to produce a substantial X-ray continuum.

Finally, our results can be compared with those on other weakly accreting AGNs observed so far by *NuSTAR*, namely NGC 5506 (estimated Eddington ratio as low as 0.7×10^{-2}; see Matt et al. 2015)[1] and NGC 2110 (estimated Eddington ratio of 0.25–3.7×10^{-2}; see Marinucci et al. 2015). Matt et al. (2015) found a lower limit on the high-energy cut-off of ∼500 keV for NGC 5506, while Marinucci et al. (2015) inferred $E_c > 210$ keV for NGC 2110. In these objects, then, a weak disc emission may be accompanied by a relatively high coronal temperature, in agreement with our present work on NGC 7213. The number of observed sources with good measurements of the high-energy cut-off is too small to establish any statistical correlation with other parameters. However, if the X-ray emission is due to a Comptonizing corona, a high coronal temperature is expected when the disc radiation is weak, because inverse Compton scattering is inefficient in cooling the corona. Further studies on a greater number of sources will be required to confirm this scenario by constraining the physical parameters of the disc/corona system.

ACKNOWLEDGEMENTS

We thank the anonymous referee for his/her helpful comments, which improved the manuscript. FU thanks Pierre-Olivier Petrucci for useful discussions and comments. This work is based on observations obtained with the *NuSTAR* mission, a project led by the California Institute of Technology, managed by the Jet Propulsion Laboratory and funded by NASA. This research has made use of data, software and/or web tools obtained from NASA's High Energy Astrophysics Science Archive Research Center (HEASARC), a service of Goddard Space Flight Center and the Smithsonian Astrophysical Observatory. FU, GM and SB acknowledge support from the French-Italian International Project of Scientific Collaboration: PICS-INAF project number 181542. FU acknowledges support from CNES and Université Franco-Italienne (Vinci PhD fellowship). FU, AM and GM acknowledge financial support from the Italian Space Agency under grant ASI/INAF I/037/12/0-011/13. SB acknowledges financial support from the Italian Space Agency under grant ASI-INAF I/037/12/P1. PA acknowledges support from FONDECYT 1140304. FEB acknowledges support from CONICYT-Chile (Basal-CATA PFB-06/2007, FONDECYT 1141218, 'EMBIGGEN' Anillo ACT1101) and the Ministry of Economy, Development, and Tourism's Millennium Science Initiative through grant IC120009, awarded to The Millennium Institute of Astrophysics, MAS.

[1] This value of the Eddington ratio is obtained by assuming the highest estimate of the black hole mass in NGC 5506, namely $\sim 10^8$ $M_\odot$. The mass is poorly known, with a lower limit of a few $\times 10^6$ $M_\odot$ (see Guainazzi et al. 2010), which would yield an Eddington ratio above 0.1.

REFERENCES

Arnaud K. A., 1996, in Jacoby G. H., Barnes J., eds, ASP Conf. Ser. Vol. 101, Astronomical Data Analysis Software and Systems V. Astron. Soc. Pac., San Francisco, p. 17
Ballantyne D. R. et al., 2014, ApJ, 794, 62
Balmaverde B., Capetti A., 2014, A&A, 563, A119
Baloković M. et al., 2015, ApJ, 800, 62
Baumgartner W. H., Tueller J., Markwardt C. B., Skinner G. K., Barthelmy S., Mushotzky R. F., Evans P. A., Gehrels N., 2013, ApJS, 207, 19
Bell M. E. et al., 2011, MNRAS, 411, 402
Beloborodov A. M., 1999, ApJ, 510, L123
Bianchi S., Matt G., Balestra I., Perola G. C., 2003, A&A, 407, L21
Bianchi S., La Franca F., Matt G., Guainazzi M., Jimenez Bailón E., Longinotti A. L., Nicastro F., Pentericci L., 2008, MNRAS, 389, L52
Blank D. L., Harnett J. I., Jones P. A., 2005, MNRAS, 356, 734
Brenneman L. W. et al., 2014, ApJ, 788, 61
Dickey J. M., Lockman F. J., 1990, ARA&A, 28, 215
Draine B. T., 2003, ApJ, 598, 1026
Elitzur M., Shlosman I., 2006, ApJ, 648, L101
Emmanoulopoulos D., Papadakis I. E., McHardy I. M., Arévalo P., Calvelo D. E., Uttley P., 2012, MNRAS, 424, 1327
Emmanoulopoulos D., Papadakis I. E., Nicastro F., McHardy I. M., 2013, MNRAS, 429, 3439
Fabian A. C., Parker M. L., Wilkins D. R., Miller J. M., Kara E., Reynolds C. S., Dauser T., 2014, MNRAS, 439, 2307
Filippenko A. V., Halpern J. P., 1984, ApJ, 285, 458
Gohil R., Ballantyne D. R., 2015, MNRAS, 449, 1449
Grier C. J. et al., 2013, ApJ, 773, 90
Gu M., Cao X., 2009, MNRAS, 399, 349
Guainazzi M., Bianchi S., Matt G., Dadina M., Kaastra J., Malzac J., Risaliti G., 2010, MNRAS, 406, 2013
Haardt F., Maraschi L., 1991, ApJ, 380, L51
Haardt F., Maraschi L., Ghisellini G., 1994, ApJ, 432, L95
Haardt F., Maraschi L., Ghisellini G., 1997, ApJ, 476, 620
Harrison F. A. et al., 2013, ApJ, 770, 103
Ho L. C., 2008, ARA&A, 46, 475
Ho L. C., 2009, ApJ, 699, 626
Hönig S. F., Beckert T., 2007, MNRAS, 380, 1172
Hönig S. F., Kishimoto M., Gandhi P., Smette A., Asmus D., Duschl W., Polletta M., Weigelt G., 2010, A&A, 515, A23
Kaspi S., Maoz D., Netzer H., Peterson B. M., Vestergaard M., Jannuzi B. T., 2005, ApJ, 629, 61
Kollmeier J. A. et al., 2006, ApJ, 648, 128
Lobban A. P., Reeves J. N., Porquet D., Braito V., Markowitz A., Miller L., Turner T. J., 2010, MNRAS, 408, 551
Lohfink A. M. et al., 2013, ApJ, 772, 83
Magdziarz P., Zdziarski A. A., 1995, MNRAS, 273, 837
Malizia A., Molina M., Bassani L., Stephen J. B., Bazzano A., Ubertini P., Bird A. J., 2014, ApJ, 782, L25
Malzac J., Beloborodov A. M., Poutanen J., 2001, MNRAS, 326, 417
Maoz D., 2007, MNRAS, 377, 1696
Marconi A., Risaliti G., Gilli R., Hunt L. K., Maiolino R., Salvati M., 2004, MNRAS, 351, 169
Marinucci A. et al., 2014, MNRAS, 440, 2347
Marinucci A. et al., 2015, MNRAS, 447, 160
Matt G. et al., 2015, MNRAS, 447, 3029
Merloni A., Fabian A. C., 2002, MNRAS, 332, 165
Murphy K. D., Yaqoob T., 2009, MNRAS, 397, 1549
Nandra K., George I. M., Mushotzky R. F., Turner T. J., Yaqoob T., 1997, ApJ, 477, 602

Narayan R., 2005, Ap&SS, 300, 177
Narayan R., Mahadevan R., Quataert E., 1998, in Abramowicz M. A., Björnsson G., Pringle J. E., eds, Theory of Black Hole Accretion Disks. Cambridge Univ. Press, p. 148
Narayan R., Yi I., 1994, ApJ, 428, L13
Nemmen R. S., Storchi-Bergmann T., Eracleous M., 2014, MNRAS, 438, 2804
Panessa F., Bassani L., Cappi M., Dadina M., Barcons X., Carrera F. J., Ho L. C., Iwasawa K., 2006, A&A, 455, 173
Pereira-Santaella M., Diamond-Stanic A. M., Alonso-Herrero A., Rieke G. H., 2010, ApJ, 725, 2270
Perola G. C., Matt G., Cappi M., Fiore F., Guainazzi M., Maraschi L., Petrucci P. O., Piro L., 2002, A&A, 389, 802
Peterson B. M. et al., 2004, ApJ, 613, 682
Petrucci P.-O. et al., 2013, A&A, 549, A73
Phillips M. M., 1979, ApJ, 227, L121
Poutanen J., Svensson R., 1996, ApJ, 470, 249
Quataert E., Di Matteo T., Narayan R., Ho L. C., 1999, ApJ, 525, L89
Reynolds C. et al., 2014, preprint (arXiv:1412.1177)
Ruschel-Dutra D., Pastoriza M., Riffel R., Sales D. A., Winge C., 2014, MNRAS, 438, 3434
Shakura N. I., Sunyaev R. A., 1973, A&A, 24, 337
Sobolewska M. A., Papadakis I. E., 2009, MNRAS, 399, 1597
Starling R. L. C., Page M. J., Branduardi-Raymont G., Breeveld A. A., Soria R., Wu K., 2005, MNRAS, 356, 727
Stern B. E., Poutanen J., Svensson R., Sikora M., Begelman M. C., 1995, ApJ, 449, L13
Svensson R., Zdziarski A. A., 1994, ApJ, 436, 599
Ursini F. et al., 2015, A&A, 577, A38
Walton D. J., Nardini E., Fabian A. C., Gallo L. C., Reis R. C., 2013, MNRAS, 428, 2901
Woo J.-H., Urry C. M., 2002, ApJ, 579, 530
Wu Q., Gu M., 2008, ApJ, 682, 212
Wu C.-C., Boggess A., Gull T. R., 1983, ApJ, 266, 28
Yaqoob T., 2012, MNRAS, 423, 3360
Yu Z., Yuan F., Ho L. C., 2011, ApJ, 726, 87
Yuan F., Zdziarski A. A., 2004, MNRAS, 354, 953
Zdziarski A. A., Lubiński P., Gilfanov M., Revnivtsev M., 2003, MNRAS, 342, 355

This paper has been typeset from a TEX/LATEX file prepared by the author.